Radius studies of ^{8}Li and ^{8}B using the optical-limit Glauber model in conjunction with relativistic mean-field theory*

FAN Guang-Wei(樊广伟)[1,2] XU Wang(徐望)[1,3;1)] M. Fukuda[4] PAN Qiang-Yan(潘强岩)[1]
CAI Xiao-Lu(蔡晓鹭)[1,2] FAN Gong-Tao(范功涛)[1,2] LI Yong-Jiang(李永江)[1,2] LUO Wen(罗文)[1,2]
XU Ben-Ji(徐本基)[1] YAN Zhe(阎喆)[1,2] YANG Li-Feng(杨利峰)[1,2]

[1] Shanghai Institute of Applied Physics, Chinese Academy of Sciences, Shanghai 201800, China
[2] Graduate University of Chinese Academy of Sciences, Beijing 100049, China
[3] University of Science and Technology of China, Hefei 230026, China
[4] Graduate School of Science Faculty of Science, Osaka University, Osaka 560-0043, Japan

Abstract We study the reaction cross sections ($\sigma_{\rm R}$) and root-mean-square (RMS) radii of ^{8}Li and ^{8}B, the halo-like nuclei, with stable target ^{12}C, ^{27}Al and ^{9}Be within the standard optical-limit Glauber model, using densities obtained from relativistic mean-field (RMF) formalisms and other types of distributions. It is found that the experimental $\sigma_{\rm R}$ can be reproduced well at high energy. The RMS radius and Δr extracted by RMF-theory and harmonic oscillator distribution are compared. We find that the RMS radius and Δr of ^{8}B are larger than those of ^{8}Li. In addition, we analyze in detail the relationship between $\sigma_{\rm R}$ and density distribution.

Key words Glauber model, root-mean-square radius, relativistic-mean-field theory, reaction cross sections

PACS 21.10.Gv, 24.10.Jv, 25.60.-t

1 Introduction

The nuclear size and density distribution are important bulk properties of nuclei which determine the nuclear potential, single-particle orbitals, wave functions, and so on. So it is very important to get the precise values for the nuclear size and density distribution.

Since the 1980s, as significant progress in accelerator technology has been made, radioactive ion beams (RIBs) have been used widely for studying structures and properties of isotopes near and far away from β-stability. The quantities measured in studies include various inclusive cross sections, such as reaction or interaction cross sections, nucleon-removal cross sections, coulomb breakup cross sections and momentum distributions of a fragment. Among these, the reaction cross section (interaction cross section at high energy [1]) is one of the most fundamental quantities characterizing nuclear reactions and to probe for nuclear structure details. In 1985, I. Tanihata et al. [2] found the neutron halo nucleus ^{11}Li by measuring the interaction cross section in the relativistic energy region. Later on, many experiments confirmed this result. However, ^{8}B multipole moment measurements, indicating a halo structure due to the weakly bound ($E_{\rm s}$=0.137 MeV) p-wave valence proton [3], triggered a set of experimental studies devoted to ^{8}B structure investigations. All of those experiments found a large reaction cross section, a relatively narrow momentum distribution of the ^{7}Be fragments and a large one-proton removal cross section, thus confirming the halo-like structure of ^{8}B. However, the matter radius has not been found to be anomalously large compared to the neighboring nuclei, and it is important to note that these experimental results seem not to be consistent. The values of the RMS radius from different experiments vary from 2.39 to 2.74 fm, which is a difference of almost 15% [4–6]. The same problem occurs with its mirror nucleus, ^{8}Li, which has a

Received 11 December 2009

* Supported by One Hundred Person Project of Chinese Academy of Sciences (26010701), Knowledge Innovation Project of Chinese Academy of Sciences (KJCX2-SW-N13, KJCX3-SYW-N2) and National Natural Science Foundation of China (10675156)

1) E-mail: wangxu@sinap.ac.cn

valence neutron with a separation energy of 2 MeV. The thickness of the neutron skin obtained by different methods ranges from 0.18 to 0.56 fm [7, 8].

Although we have no straightforward model-independent method for determining the matter-density distribution of unstable nuclei now, the Glauber model has been used extensively. It is based on the independent individual nucleon-nucleon collisions in the overlap zone of the colliding nuclei, accounting for a significant part of the breakup effects that play an important role in the reaction of a weakly bound nucleus, and successfully explains the observed nuclear reaction cross section for various systems at high energies. Although the model is simple, it shows reasonable results in many cases. This model requires the structural information, namely the density distribution, of the nuclei involved (projectile and target) and N-N cross section. The structural information has to be provided by nuclear structure models, like the Harmonic-oscillator-type (HO-type) distribution and the Gaussian distribution. In this work, beside these two distributions, we also use the RMF-theory as involved nuclear structure calculations to reproduce the $\sigma_{\rm R}$. The free N-N cross sections are inappropriate, however, because the effective values may differ from the free-nucleon values due to nuclear-matter effects and Fermi-motion [2, 9]. To determine the effective N-N cross sections, we use a HO-type distribution of ^{12}C and take $\sigma_{\rm R}$ of ^{12}C+^{12}C as a calibration. The reason why we use a HO-type distribution and $\sigma_{\rm R}$ of ^{12}C will be explained below. The obtained value is 71% of the free N-N cross sections.

The main objective of the present work is to study the RMS radii and Δr ($R_{\rm n,p} - R_{\rm p,n}$ for ^{8}Li and ^{8}B) of ^{8}Li, and ^{8}B and to extract the density distribution of ^{12}C, ^{9}Be and ^{27}Al, which in July 2009 were used as experimental targets for ^{8}Li in HIMAC. This article is presented as follows. In Sec. 2, we discuss in brief the formalism used in the present work. In Sec. 3, we extract the effective N-N cross section and the density distributions of the stable targets ^{12}C, ^{27}Al and ^{9}Be. In Sec. 4, we discuss the RMS radii of ^{8}Li and ^{8}B using RMF-theory in conjunction with the Glauber model. The summary and conclusion are given in Sec. 5.

2 Formalism

2.1 Glauber model

The standard Glauber model form for the reaction cross section, given by R. J. Glauber[10], is deduced from the eikonal approximation given by

$$\sigma_{\rm R} = 2\pi \int_0^\infty b[1-T(b)]{\rm d}b, \quad (1)$$

where $T(b)$ is the transmission as a function of the impact parameter b. A straightforward calculation of $T(b)$ is complicated. One of the simplest approximations to calculate $T(b)$ is the optical limit. In this approximation we get

$$T(b) = \exp\left\{-\sum_{i,j}\sigma_{ij}\int \rho^z_{Ti}\rho^z_{pj}(|b-z|){\rm d}s\right\}. \quad (2)$$

Here, $\rho^z_{Ki}(s)$ is an over the z-direction integrated nucleon-density distribution,

$$\rho^z_{Ki}(s) = \int_{-\infty}^{\infty} \rho_{Ki}(\sqrt{s^2+z^2}){\rm d}z, \quad (3)$$

where the index $k = P$ (projectile) or T (target) means projectile or target nucleon-density distribution and σ_{ij} are the N-N cross sections, used to replace the profile function in the zero range limits, in which the indices i, j are used to distinguish protons and neutrons.

This model is successful in reproducing reaction cross sections for various systems at high energy [11]. To explain its success at high energy in more detail, we perform an analysis by comparing the $\sigma_{\rm R}$ derived with a Gaussian distribution and a HO-type distribution of ^{12}C extracted in this work. Fig. 1 and Fig. 2 show us that the reaction cross sections at high energy, for example the (b) in Fig. 1 and Fig. 2, are mainly depend on the core-nucleons and the reaction cross sections at low energy, for example the (d) in Fig. 1 and Fig. 2 are sensitive to outer-nucleons. If peripheral distribution changes by 2%, the reaction cross sections show a 6.5% difference at low energy. At the same time, the RMS radii differ by 1%. So we can use it to discuss the RMS radii and Δr of ^{8}Li and ^{8}B at high energy.

2.2 Nuclear structure models

To get the structure information, we employ three types of density distributions: HO-type distribution, Gaussian distribution and RMF-theory, which recently has been effectively used for this purpose [12]. The HO-type and the Gaussian distributions each have one size parameter. We get these parameters through experimental data: reaction cross sections and charge-RMS radius. For ^{8}B, we get the RMS radius by using a HO-type distribution based on the Gaussian calculation. The RMF theory has several sets of parameters to calculate the density distribution which we will use in this paper. For details, see Ref. [13].

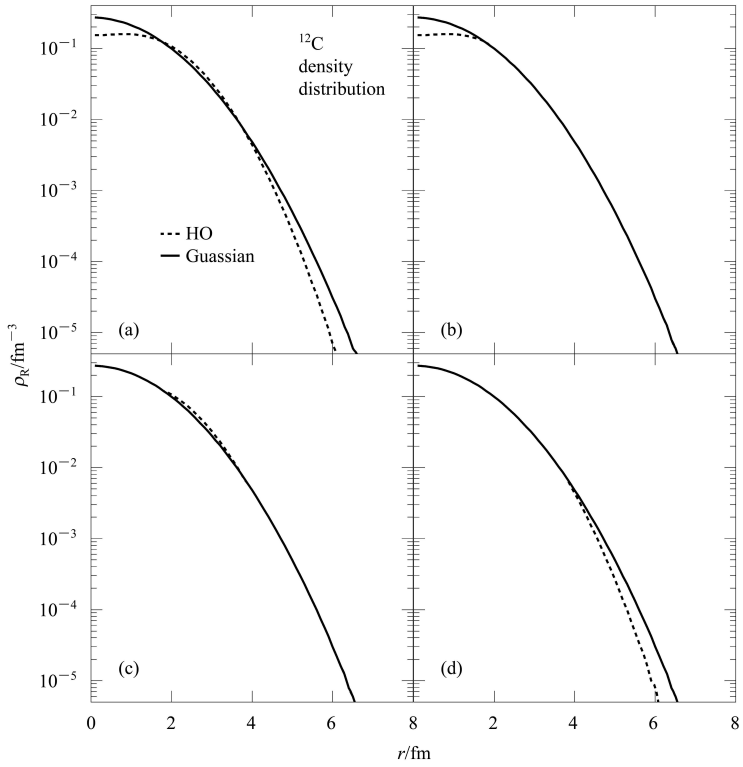

Fig. 1. Comparison of density distribution obtained from HO-type and Gaussian distribution. (a) shows the density distribution of ^{12}C, (b) shows the difference between core-nucleon in (a). The purpose of (c) and (d) are the same with (b) to show one aspect difference of (a).

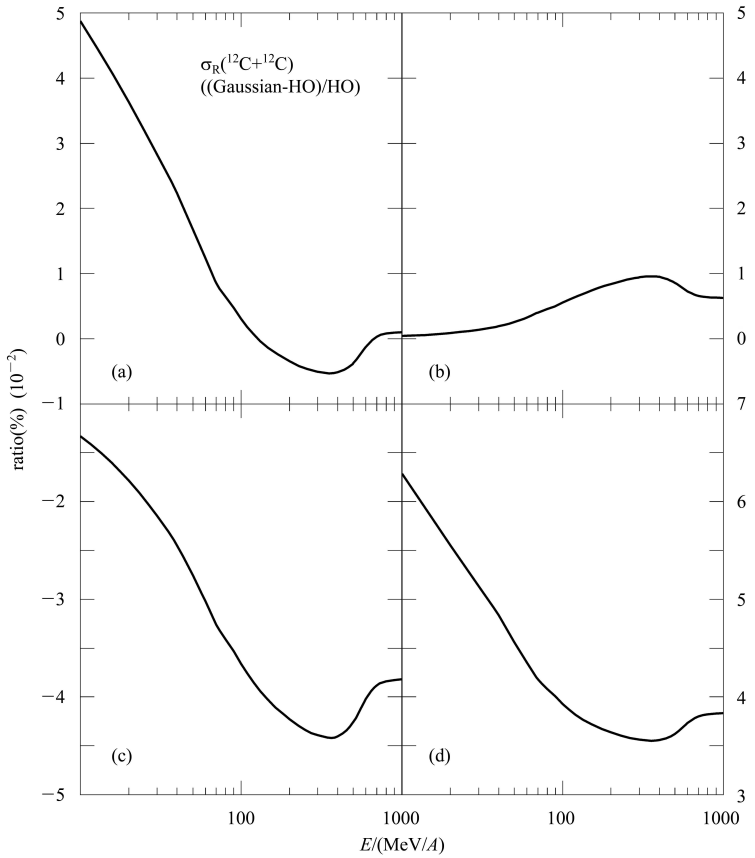

Fig. 2. Ratios of reaction cross sections. (a), (b), (c) and (d) correspond to Fig. 1.

The HO-type density distribution as a useful model is successful in explaining stable nuclei even such as ^{48}Ca and ^{208}Pb [14]. On the other hand, for light stable nuclei ($A \leqslant 20$), the HO-type density distribution is sufficient to describe the experimental data. The HO-type density distributions including the contributions up to the sd-shell are given by the following equations,

For $2< Z <8$, $2 < N <8$:

$$\rho_{\rm n}(r) = 2\pi^{-\frac{3}{2}}\lambda^{-3}\left(1-\frac{1}{A}\right)^{-\frac{3}{2}}{\rm e}^{-x^2}\left(1+\frac{N+2}{3x^2}\right). \quad (4)$$

$$\rho_{\rm p}(r) = 2\pi^{-\frac{3}{2}}\lambda^{-3}\left(1-\frac{1}{A}\right)^{-\frac{3}{2}}{\rm e}^{-x^2}\left(1+\frac{Z+2}{3x^2}\right). \quad (5)$$

For $2> Z >8$, $2> N >8$:

$$\rho_{\rm n}(r) = 4\pi^{-\frac{3}{2}}\lambda^{-3}\left(1-\frac{1}{A}\right)^{-\frac{3}{2}}\frac{N}{N+8}{\rm e}^{-2} \times\left(1+2X^2\frac{N-8}{15x^4}\right). \quad (6)$$

$$\rho_{\rm p}(r) = 4\pi^{-\frac{3}{2}}\lambda^{-3}\left(1-\frac{1}{A}\right)^{-\frac{3}{2}}\frac{Z}{Z+8}{\rm e}^{-2} \times\left(1+2X^2\frac{Z-8}{15x^4}\right). \quad (7)$$

Here, A, N and Z are the mass, neutron and proton numbers, $x^2=\left(\frac{r}{\lambda}\right)^2$ and λ denotes the size parameter.

The Gaussian calculation uses

$$\rho_k(r) = x_k \exp\left\{\left[-\left(\frac{r}{b}\right)^2\right]\right\}. \quad (8)$$

The index k denotes a proton or a neutron, and x_k and b are the amplitude and width respectively.

3 Density distribution of ^{12}C, ^{27}Al and ^{9}Be, the RMS radii of ^{8}Li and ^{8}B

As a calibration, ^{12}C was measured by many experiments. The collected data are listed in the Table 1. The last one of 2.464±0.009 fm is the normalized result from these data by the equation

$$\sum\frac{A_i}{x_i^2}\Big/\sum\frac{1}{x_i^2},$$

where x_i^2 and A_i are experimental radii and errors. We use this value as ^{12}C charge-RMS to get the effective N-N cross sections. In Table 2, we show the results calculated with the Gaussian and HO-type distribution. In Table 3, we show the results obtained from the RMF-theory. Reaction cross sections calculated with the Glauber model in conjunction with RMF-theory are listed in Table 4.

The $R_{\rm m}$ is obtained by calculations with a Gaussian distribution and with a HO-type distribution differ by about 1%. There are two major reasons for this: (Ⅰ) there is a 2% difference in the outer-nucleon distribution in these two kinds of calculation, (Ⅱ) the total cross sections for proton-proton,

Table 1. Charge-RMS radii of ^{12}C, and ^{27}Al. The last one is the normalized result.

$R_{\rm c}(^{12}{\rm C})$/fm	Ref.	$R_{\rm c}(^{27}{\rm Al})$/fm	Ref.
2.46±0.025	[15]	3.06±0.09	[24]
2.453±0.008	[16]	3.05±0.05	[18]
2.468±0.016	[17]	3.035±0.040	[25]
2.462±0.022	[18]	3.057±0.013	
2.471±0.0055	[19]	3.0554±0.0004	
2.40±0.56	[20]	3.058±0.05	[26]
2.32±0.16	[21]	3.0554±0.0004	
2.49±0.05	[22]		
2.472±0.016	[23]		
2.43±0.02	[2]		
2.464±0.009			

Table 2. Comparison of RMS radii obtained from a Gaussian distribution and a HO-type calculation with normalized result (see the first paragraph of Sec. 3.). $R_{\rm m}$ and $R_{\rm n}$ mean matter-RMS radius and neutron-RMS radius, respectively. The parameters of the Gaussian distribution extracted here are ^{12}C(1.99, 1.0), ^{27}Al(2.451, 1.0) and ^{9}Be (2.06, 1.0), which have been normalized first. The parameters of the HO-type distribution extracted here are ^{12}C (1.7485, 1.7485), ^{27}Al (1.9505, 1,98) and ^{9}Be (1.889, 1.878). The first value is for protons. The RMS radii of ^{9}Be and ^{8}Li are taken from Ref. [27] and Ref. [28].

nuclei	Exp.	Gaussian	Harmornic-Oscillator		
	$R_{\rm c}$/fm	$R_{\rm m}$/fm	$R_{\rm m}$/fm	$R_{\rm c}$/fm	$R_{\rm n}$/fm
^{12}C	2.464 ±0.009	2.437±0.019	2.464±0.019	2.464±0.019	2.464±0.019
^{27}Al	3.0554±0.0004	3.006±0.010	3.093±0.009	3.055±0.009	3.127±0.009
^{9}Be	2.519 ±0.012	2.523±0.022	2.545±0.020	2.519±0.020	2.566±0.020
^{8}Li	2.299 ±0.032	2.486±0.037	2.493±0.023	2.299±0.023	2.603±0.023
^{8}B		2.572±0.058	2.588±0.029	2.725±0.029	2.343±0.029

Table 3. Comparison of RMS radii of ^{8}Li and ^{8}B obtained from RMF-theory with different parameters. The experimental data of the binding energy are taken from Ref. [33].

nuclei	radius/fm			$R_{\rm n,c}-R_{\rm c,n}$/fm	Binding-Energy/MeV	
	$R_{\rm m}$	$R_{\rm c}$	$R_{\rm n}$	Δr	Calc.	Exp.
^{8}Li(NL-SH)	2.507	2.277	2.508	0.231	42.793	41.277
^{8}Li(NL1)	2.660	2.404	2.683	0.279	42.850	
^{8}Li(NLz)	2.654	2.404	2.672	0.268	44.617	
^{8}Li(TM1)	2.556	2.313	2.566	0.253	43.0	
^{8}Li(TM2)	2.522	2.284	2.527	0.243	44.408	
^{8}B(NL-SH)	2.559	2.716	2.121	0.595	38.686	37.737
^{8}B(NL1)	2.720	2.893	2.263	0.630	39.029	
^{8}B(NLz)	2.711	2.880	2.263	0.617	40.758	
^{8}B(TM1)	2.610	2.776	2.160	0.616	38.985	
^{8}B(TM2)	2.569	2.728	2.130	0.598	40.338	

Table 4. Reaction cross sections calculated with the Glauber model in combination with the RMF-theory. The experimental data are taken from Refs. [8, 34]. The energies are 790 MeV/u for ^{12}C and ^{9}Be, 285 MeV/u for ^{8}B+^{27}Al.

nuclei	$\sigma_{\rm R}(+^{12}{\rm C})$/mb		$\sigma_{\rm R}(+^{27}{\rm Al})$/mb		$\sigma_{\rm R}(+^{9}{\rm Be})$/mb	
	Calc.	Exp.	Calc.	Exp.	Calc.	Exp.
^{8}Li(NL-SH)	757.1	768±9	1142.2	1147±14	702.0	727±6
^{8}Li(NL1)	791.0		1188.1		730.0	
^{8}Li(NLz)	789.2		1186.0		729.1	
^{8}Li(TM1)	768.1		1157.3		710.9	
^{8}Li(TM2)	760.7		1146.9		704.9	
^{8}B(NL-SH)	775.8	784±14	1050.2	1110±7	714.5	731±15
^{8}B(NL1)	810.9		1090.7		743.5	
^{8}B(NLz)	809.1		1088.4		742.1	
^{8}B(TM1)	786.9		1063.1		723.5	
^{8}B(TM2)	778.2		1171.6		716.6	

neutron-neutron and proton-neutron scattering are not the same in the two systems ^{27}Al and ^{9}Be [9]. The $R_{\rm m}$ and Δr of ^{8}B are larger than those of ^{8}Li by about 3.8% ± 1.5% and 25.7% ± 15.2%, respectively.

4 The RMS radii of ^{8}Li and ^{8}B using RMF-theory in combination with the Glauber model

The RMF-theory, which naturally includes the strong three-body repulsion, responsible for the saturation, and a strong spin-orbit force which is responsible for the magic numbers, has gained considerable success in describing various facets of nuclear structure properties. For instance, it leads to a quantitative description of the binding energy and equilibrium density of nuclear matter. With a very limited number of parameters, it is also able to give a quantitative description of the ground-state properties at and off the stability line [29, 30]. Because of the success of

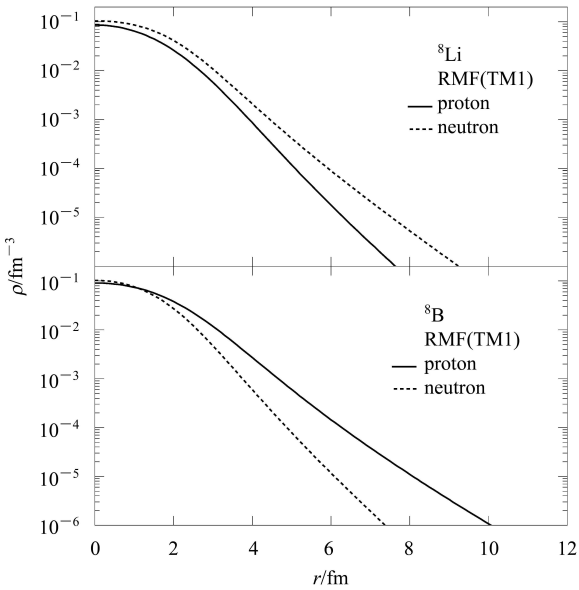

Fig. 3. Density distributions of ^{8}Li and ^{8}B obtained from RMF-theory. The solid line and dashed line represent protons and neutrons, respectively.

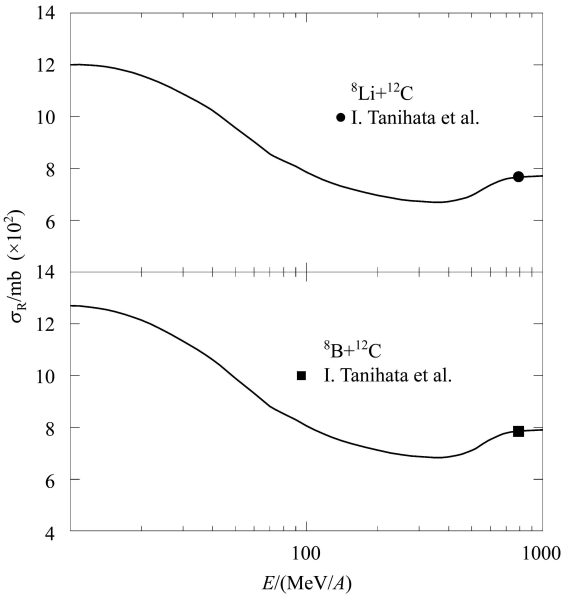

Fig. 4. Reaction cross sections of ^{8}Li and ^{8}B calculated by the Glauber model in conjunction with RMF-theory.

both theories, Glauber model and RMF-theory, we combine them in order to study $\sigma_{\rm R}$ and the RMS-radii of ^{8}Li and ^{8}B. For TM1, $R_{\rm m}$ and Δr of ^{8}B is larger than ^{8}Li by about 2.1% and 143.5%, respectively. For TM2, these values are 1.9% and 146.1%, respectively. The results are listed in Table 3 and Table 4. We also show results in Fig. 3 and Fig. 4. For information about the parameters TM1 and TM2, see Refs. [31] and [32].

5 Summary

In summary, we studied the RMS radii of ^{8}Li and ^{8}B in the framework of the Glauber model with densities obtained from Gaussian, HO-type distribution and RMF-theory. We studied in detail the relationship between densities and $\sigma_{\rm R}$. Comparing the results obtained with the RMF-theory using different parameters showed that $\sigma_{\rm R}$ can be reproduced well with a combination of the Glauber model and the RMF-theory (TM1, TM2) at high energy. We found that $R_{\rm m}$ and Δr of ^{8}B are larger than those of ^{8}Li, but no decision is yet possible as to whether ^{8}Li is a halo or a skin-nucleus yet. In July 2009, further studies at low energies were started at HIMAC. We hope to be able to present in the future results for its charge and neutron density distribution by using a modified Glauber Model [9].

The authors want to thank Prof. Ren Zhong-Zhou (NJU) for providing the RMF-theory code, and Associate Researcher Fang De-Qing (SINAP) for his help with this subject.

References

1 Kohama A, Iida K, Oyamatsu K et al. Phys. Rev. C, 2008, **78**: 061601
2 Tanihata I, Hamagaki H, Hashimoto O et al. Phys. Rev. L, 1985, **55**: 2676
3 Minamisono T, Ohtsubo T, Minami I et al. Phys. Rev. L, 1992, **69**: 2058
4 Warner R E, Kelley J H, Becchetti F D et al. Phys. Rev. C, 1995, **52**: 1166(R)
5 Ogawa Y, Tanihata I. Nucl. Phys. A, 1997, **616**: 239
6 Warner R E, Becchetti F D, Brown J A et al. Phys. Rev. C, 2004, **69**: 024612
7 Kitagawa H, Sagawa H. Phys. Lett. B, 1993, **299**: 1
8 Tanihata I, Kobayashi T, Yamakawa O et al. Phys. Lett. B, 1988, **206**: 592
9 Takechi M, Fukuda M, Mihara M et al. Phys. Rev. C, 2009, **79**: 061601(R)
10 Glauber R J. Lectures in Theoretical Physics. Edited by Brittin W E, Dunham L G Interscience, New York, 1959 315
11 Bertsch G F, Brown B A. Phys. Rev. C, 1989, **39**: 1154
12 Shukla A, Sharma B K, Chandra R et al. Phys. Rev. C, 2007, **76**: 034601
13 Reinhard P G. Rep. Prog. Phys., 1989, **52**: 439
14 Ozawa A, Suzuki T, Tanihata I. Nucl. Phys. A, 2001, **693**: 32
15 Sick I, McCarthy J S. Nucl. Phys. A, 1970, **150**: 631
16 Jansen J A, Peerdeman R T, Vries D. Nucl. Phys. A, 1972, **188**: 337
17 Sick I. Phys. Lett. B, 1973, **44**: 62
18 Fey G, Frank H, Theissen H. Z. Phys., 1973, **265**: 401
19 Sick I. Phys. Lett. B, 1982, **116**: 212
20 Backenstoss G, Claralambus S, Daniel H et al. Phys. Lett. B, 1967, **25**: 547
21 Barrett R C. Phys. Lett. B, 1970, **33**: 388
22 Dubler T, Schellenberg L, Schneuwly H et al. Nucl. Phys. A, 1974, **219**: 29
23 Schaller L A et al. Nucl. Phys. A, 1978, **379**: 324
24 Lombard R M and Bishop R. Nucl. Phys. A, 1967, **101**: 601
25 Fricke G, Herberz J, Hennemann T et al. Phys. Rev. C, 1992, **45**: 80
26 Schaller L A. Nucl. Phys. A, 1978, **300**: 225
27 Nortershäüser W, Tiedemann D, Žáková M et al. Phys. Rev. L, 2009, **102**: 062503
28 Sánchez R, Nörtershäuser W, Ewald G et al. Phys. Rev. L, 2006, **96**: 033002
29 REN Zhong-Zhou, CHEN Bao-Qiu, XU Gong-Ou. Phys. Rev. C, 1996, **53**: R572
30 REN Zhong-Zhou, Faessler Amand, Bobyk A. Phys. Rev. C, 1998, **57**: 2752
31 WANG Zai-Jun, REN Zhong-Zhou. Phys. Rev. C, 2004, **70**: 034303
32 REN Zhong-Zhou, MAO Y C, ZHI Q J. Jornal of Radioanalytical and Nuclear Chemistry, 2007, **272**: 209–213
33 Audi G, Wapstra A H, Thibault C. Nucl. Phys. A, 2003, **729**: 337
34 Blank B, Marchand C, Pravikoff M S et al. Nucl. Phys. A, 1997, **624**: 242